

# The Mystery of Two Straight Lines in Bacterial Genome Statistics. Release 2005

Alexander Gorban\*

Centre for Mathematical Modelling,

University of Leicester, UK

and Institute for Computational Modelling

Russian Academy of Sciences, Krasnoyarsk, Russia

Andrey Zinovyev†

Institut des Hautes Études Scientifiques,

Bures-sur-Yvette, France

and Institut Curie, Paris, France

## Abstract

In special coordinates (codon position-specific nucleotide frequencies) bacterial genomes form two straight lines in 9-dimensional space: one line for eubacterial genomes, another for archaeal genomes. All the 175 known bacterial genomes (Genbank, March 2005) belong these lines with high accuracy, and these two lines are certainly different. The results of PCA analysis of codon usage and accuracy of mean-field (context-free) approximation are presented. The first two principal components correlate strongly with genomic G+C-content and the optimal growth temperature respectively. The variation of codon usage along the third component is related to the curvature of the mean-field approximation. The eubacterial and archaeal genomes codon usage are clearly distributed along two third order curves with genomic G+C-content as a parameter.

## 1 Introduction

In this paper we present results of statistical analysis of the set of known bacterial genomes (175 bacterial genomes from Genbank release March 2005). In some sense these results are experimental ones: we analyze the experimental data from Genbank without additional theoretical hypothesis.

---

\*ag153@le.ac.uk

†zinovyev@ihes.fr

For statistical analysis of various genomes it is necessary to represent each genome as a point in euclidian space. The distinguished way for such a representation give us statistical *frequency dictionaries*: coordinates are the frequencies of words in the four-letter alphabet (A, C, G, T). The simplest examples give us the famous *codon usage* and the *codon position-specific nucleotide frequencies*. The space of codon usage is 63-dimensional standard simplex in 64-dimensional Euclidean space, and dimension of the space of codon position-specific nucleotide frequencies is 9 (12 frequencies minus 3 normalization condition). In these spaces the bacterial genomes form two lines. These lines can be parametrized by one parameter, the average genomic CG-content. For lines in the codone usage space an approximation of 3d order has appropriate accuracy, and the lines in the space of codon position-specific nucleotide frequencies represent the linear functions of the average genomic CG-content. The observed “dimension reduction” (lines instead of multidimensional clouds) can serve as a starting point for “selection-mutations” theories.

Some slices and particular cases of these “genome trajectories” are known and serve as important arguments in the proof of the genome code universality [1]. Now we prove universality of this phenomenon, and can formulate a challenge for theoretical study: why the bacterial genomes form these trajectories with so high accuracy?

## 2 Results

For each genome we can define the *codon position-specific nucleotide frequencies* in the coding part of this genome. The coding part of the genome is divided into codons. The codon position-specific nucleotide frequencies are 12 numbers  $p_{\alpha}^i$ , where  $\alpha$  is a nucleotide symbol (A, C, G, or T), and  $i = 1, 2, 3$  is a position number of nucleotide in codon. Among 12 frequencies  $p_{\alpha}^i$  only 9 are independent because of the normalization conditions  $p_A^i + p_C^i + p_G^i + p_T^i = 1$ . The possibility of non-uniqueness of separation of the coding part into codons is here neglected. The vectors with all possible coordinates  $p_{\alpha}^i$  fill a 9-dimensional polyhedron (a direct sum of three 3-dimensional symplexes). In this 9-dimensional space bacterial genomes form two straight lines: one line for eubacterial genomes, another for archaeal genomes. All the 175 known bacterial genomes (from Genbank release March 2005) belong these lines with high accuracy, and these two lines are certainly different. Both these lines can be parametrized by G+C genomic content in a very natural way, because  $p_{\alpha}^i$  prove to be linear functions of (non position-specific) G+C content with high accuracy. These functions are different for different lines. The results of statistical analysis (the regression lines together with experimental points) are presented in Fig. 1. Significant differences between eubacteria and arhaea are observed for  $p_A^1$ ,  $p_G^3$ ,  $p_T^2$ , and  $p_T^3$  functions (see Table 1 with intervals for 90% confidence level).

The average *codon usage* (*cu*) in genome is represented by 64 frequencies  $p_{\alpha\beta\gamma}$ , where  $\alpha$ ,  $\beta$ , and  $\gamma$  are nucleotide symbols,  $p_{\alpha\beta\gamma}$  is the frequency of the codon  $\alpha\beta\gamma$  in coding part of genome. The *mean-field* approximation (*mf*) for codon usage is  $p_{\alpha\beta\gamma}^M = p_{\alpha}^1 p_{\beta}^2 p_{\gamma}^3$ . The frequencies  $p_{\alpha\beta\gamma}^M$  for bacterial genomes belong to lines of third

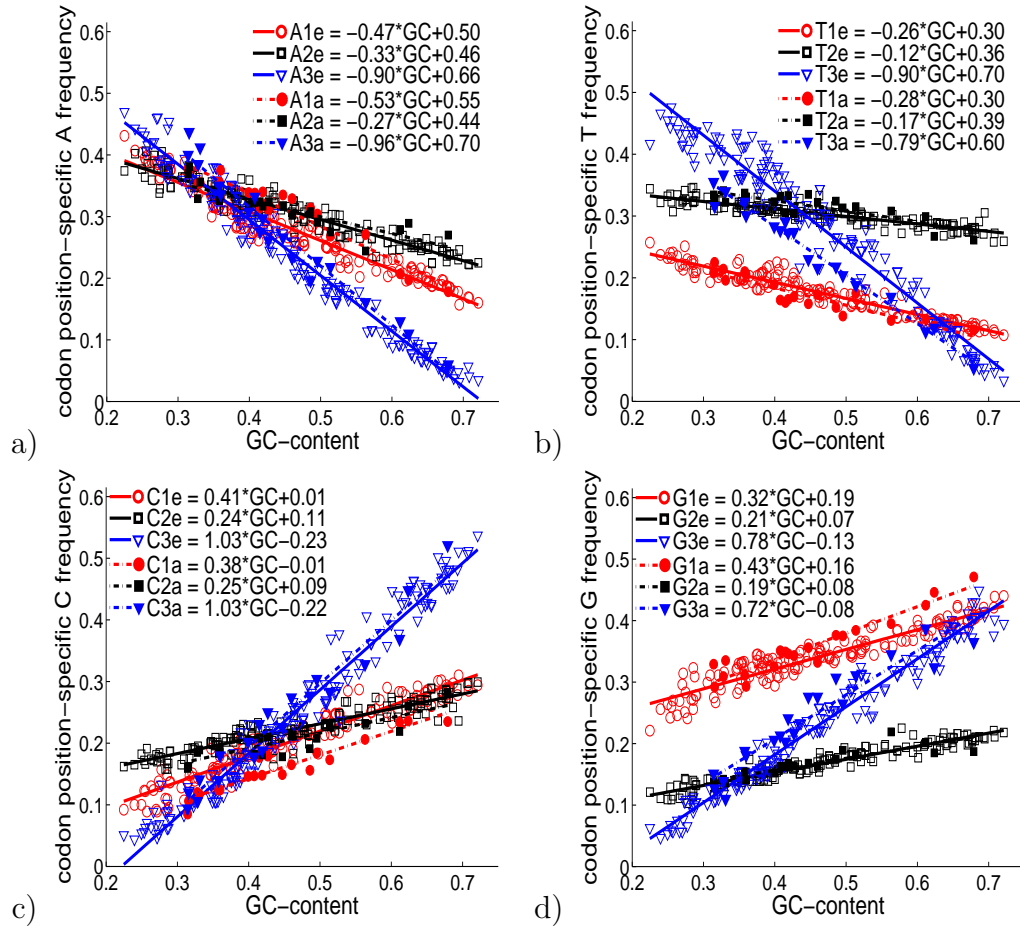


Figure 1: Codon position-specific nucleotide frequencies as functions of average G+C-content. Solid line and empty points correspond to 155 completed eubacterial genomes, broken line and filled points correspond to 20 completed archaeal genomes.

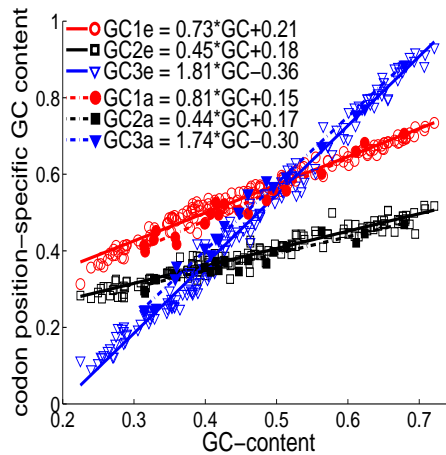


Figure 2: Position-specific G+C-content as functions of average G+C-content. Solid line and empty points correspond to 155 completed eubacterial genomes, broken line and filled points correspond to 20 completed archaeal genomes.

Table 1: Coefficients for  $p_{\bullet}(GC) = k_1 + k_2 \times GC$  regression with intervals for 90% confidence level.  $R^2$  statistics shows how much variation is explained by regression.

Function	$k_1$	$k_2$	$k_1$ interval	$k_2$ interval	$R^2$	$p$ -value
EUBACTERIA						
A1	0.50	-0.47	(0.488;0.505)	(-0.490;-0.454)	0.928	0
A2	0.46	-0.33	(0.455;0.468)	(-0.347;-0.320)	0.915	0
A3	0.66	-0.90	(0.645;0.666)	(-0.923;-0.882)	0.971	0
C1	0.01	0.41	(0.005;0.021)	(0.396;0.431)	0.913	0
C2	0.11	0.24	(0.104;0.117)	(0.229;0.255)	0.864	0
C3	-0.23	1.03	(-0.240;-0.216)	(1.003;1.054)	0.967	0
G1	0.20	0.32	(0.186;0.201)	(0.305;0.335)	0.886	0
G2	0.07	0.21	(0.064;0.072)	(0.204;0.222)	0.909	0
G3	-0.13	0.78	(-0.139;-0.121)	(0.761;0.797)	0.970	0
T1	0.30	-0.26	(0.292;0.302)	(-0.271;-0.251)	0.922	0
T2	0.36	-0.12	(0.356;0.364)	(-0.129;-0.113)	0.803	0
T3	0.70	-0.91	(0.688;0.716)	(-0.933;-0.877)	0.949	0
GC1	0.21	0.73	(0.198;0.214)	(0.717;0.750)	0.971	0
GC2	0.18	0.46	(0.171;0.187)	(0.438;0.471)	0.933	0
GC3	-0.36	1.81	(-0.371;-0.344)	(1.781;1.835)	0.988	0
ARCHAEA						
A1	0.55	-0.53	(0.522;0.579)	(-0.595;-0.471)	0.925	$1 \times 10^{-11}$
A2	0.44	-0.27	(0.407;0.465)	(-0.336;-0.210)	0.759	$6 \times 10^{-7}$
A3	0.70	-0.96	(0.662;0.734)	(-1.034;-0.879)	0.962	$3 \times 10^{-14}$
C1	-0.01	0.34	(-0.035;0.011)	(0.335;0.435)	0.908	$9 \times 10^{-11}$
C2	0.09	0.25	(0.066;0.117)	(0.195;0.305)	0.773	$3 \times 10^{-7}$
C3	-0.22	1.03	(-0.258;-0.174)	(0.934;1.117)	0.955	$2 \times 10^{-13}$
G1	0.17	0.43	(0.139;0.191)	(0.372;0.486)	0.904	$1 \times 10^{-10}$
G2	0.08	0.19	(0.060;0.099)	(0.150;0.236)	0.771	$4 \times 10^{-7}$
G3	-0.08	0.72	(-0.126;-0.035)	(0.621;0.818)	0.899	$2 \times 10^{-10}$
T1	0.30	-0.28	(0.273;0.318)	(-0.328;-0.230)	0.845	$1 \times 10^{-8}$
T2	0.39	-0.17	(0.371;0.413)	(-0.214;-0.123)	0.695	$5 \times 10^{-6}$
T3	0.60	-0.79	(0.573;0.622)	(-0.840;-0.732)	0.972	$2 \times 10^{-15}$
GC1	0.153	0.814	(0.122;0.185)	(0.746;0.883)	0.959	$6 \times 10^{-14}$
GC2	0.171	0.443	(0.145;0.196)	(0.388;0.499)	0.914	$5 \times 10^{-11}$
GC3	-0.297	1.745	(-0.333;-0.260)	(1.666;1.823)	0.988	0

order (two such lines: one for eubacterial genomes, another for archaeal genomes) in the 63-dimensional simplex of codon usage (64 frequencies minus one normalization condition) and the codon usage for known genomes form the clouds near these lines. These clouds of codon usage have a distinctive horseshoe form [3].

On Fig. 3 we show 3D PCA plot visualizing average codon usage distributions. The first two principal components have been shown (in [10]) to correlate strongly with genomic G+C-content and the optimal growth temperature respectively. The variation of codon usage along the third component was not discussed in the literature, but from Fig. 3 it seems that it is related to the curvature of the mean-field approximation manifold  $\mathbf{M}$ . The eubacterial and archaeal genomes are clearly distributed along two trajectories and we approximated them by fitting third order curves with genomic G+C-content as a parameter:

$$p_{\alpha\beta\gamma} \approx a_{\alpha\beta\gamma}GC^3 + b_{\alpha\beta\gamma}GC^2 + c_{\alpha\beta\gamma}GC + d_{\alpha\beta\gamma}, \quad (1)$$

where coefficients  $a_{\alpha\beta\gamma}, b_{\alpha\beta\gamma}, c_{\alpha\beta\gamma}, d_{\alpha\beta\gamma}$  are fitted from data separately for eubacterial and archaeal genomes. The order three is chosen because the mean-field approximations are known to be distributed along trajectories of the third order ( $p_{\alpha\beta\gamma}^M = p_{\alpha}^1(GC)p_{\beta}^2(GC)p_{\gamma}^3(GC)$ , where all dependencies on GC are close to linear, see Fig. 1). These trajectories are also shown on Fig. 3(top-right, bottom-left).

Using PCA as a visualization tool restricts us with Euclidean metrics, simultaneously giving us advantage to learn principal components on a subset of points and after project the rest onto the linear envelope of the principal vectors extracted. On Fig. 3 (bottom-left) we use this method to project both the average codon usage  $cu$  and the mean-field approximations  $mf$  onto the linear principal 3D manifold calculated for the mean-field approximations only. In this projection<sup>1</sup> one can see that, indeed, the mean-field approximation works quite nicely. But on the other linear manifold, constructed for the totality of the points, one can see that the mean-field approximations have a very particular displacement (see Fig. 3 (top-right)). This observation makes the story with mean-field approximation far from being completely trivial: one has to explain why vectors connecting  $cu$  and  $mf$  points are almost co-linear on this picture and the  $mf$  points are collected together, is it simply an artefact of projection or there is a specific direction of information loss in the 64-dimensional space? At least, it is clear that the average codon usage is not simply randomly dispersed in the vicinity of  $\mathbf{M}$ , but its ring-like spatial structure is somehow specifically oriented relatively to the mean-field approximation manifold.

### 3 Discussion

We show that the eubacterial and archaeal genomes in the 63-dimensional (64-1) space of codone usage are distributed along two trajectories that are 3d-order curves parametrized by genomic G+C-content, and in the 9-dimensional space (12-3) of

---

<sup>1</sup>In fact, this 3D manifold is almost perfectly embedded into the  $\mathbf{M}$  manifold. This means that this is a principal “view” from within  $\mathbf{M}$ .

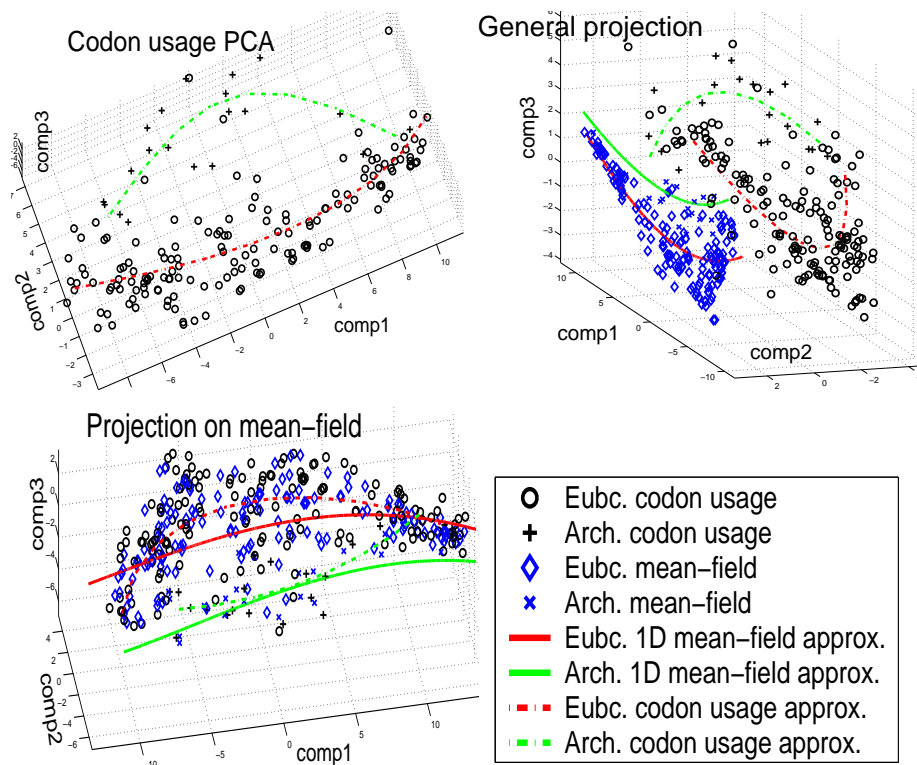


Figure 3: PCA plots for the average codon usage and the corresponding mean-field approximations for 175 bacterial genomes; top-left: PCA plot of the average codon usage; top-right: projection on the linear envelope of principal components calculated for the average codon usage and the corresponding mean-field approximations taken together; bottom-left: projection on the linear envelope of principal components calculated for the mean-field approximations only. Solid lines represent triplet frequencies calculated with use of one-dimensional approximation of mean-field approximation (see Fig. 1), stroked lines represent fitting distribution of the average codon usage using third order curves.

codon position-specific nucleotide frequencies bacterial genomes form two straight lines: one line for eubacterial genomes, another for archaeal genomes.

Some hints to observed structure were reported recently in studies on multivariate analysis of bacterial codon usage (for example, see Figure 6 from [3], or in codon bias study in [5]). Some illustrations for Genbank release 2004 can be found in our online publications [6, 7, 8] and on the web-site [9].

This observation is consistent with previous studies (Sueoka's neutrality plots, etc. [2, 11]), nevertheless, the accuracy of the linear approximations (Fig. 1) seems to be surprising. The correlation of amino-acids usage with genomic G+C-content was studied for 59 bacterial genomes [4].

The difference between linear dependencies (Fig. 1) for eubacterial and archaeal genomes is not explained yet (it is not a difference between two or several genomes, it is the difference between two straight lines which model the codon-position specific nucleotide usage with high accuracy). Available archaeal genomes are biased towards thermophilic species and they are known to have their own specific synonymous and non-synonymous codon usage [3]. The results of [10] show that synonymous codon usage is affected by two major factors: (i) the overall G+C content of the genome and (ii) growth at high temperature. It is natural to look for the source of the observed differences in these properties of thermophilic bacteria. This observation is also supported by our PCA analysis.

The first two principal components correlate strongly with genomic G+C-content and the optimal growth temperature respectively. The variation of codon usage along the third component is related to the curvature of the mean-field approximation.

The eubacterial and archaeal genomes codon usage are clearly distributed along two third order curves with genomic G+C-content as a parameter.

## References

- [1] Sueoka N., On the genetic basis of variation and heterogeneity of DNA base composition, *Proc. Natl. Acad. Sci. USA*, 48 (1962), 582–592.
- [2] Sueoka, N., Directional mutation pressure and neutral molecular evolution, *Proc. Natl. Acad. Sci. USA*, 85 (8) (1988), 2653–2657.
- [3] Lobry, J.R., Chessel, D., Internal correspondence analysis of codon and amino-acid usage in thermophilic bacteria, *J. Appl. Genet*, 44 (2) (2003), 235–261.
- [4] Lobry, J., Influence of genomic G+C content on average amino-acid composition of proteins from 59 bacterial species, *Gene*, 205(1-2) (1997), 309-316. 44 (2) (2003), 235–261.
- [5] Carbone, A., Kepes, F., Zinovyev, A., Codon Bias Signatures, Organisation of Microorganisms in Codon Space and Lifestyle. *Mol Biol Evol.* 2004 Nov 10.

- [6] Gorban, A.N., Popova, T.G., Zinovyev, A.Yu., Four basic symmetry types in the universal 7-cluster structure of 143 complete bacterial genomic sequences, e-print: <http://arxiv.org/abs/q-bio.GN/0410033> .
- [7] Gorban, A.N., Zinovyev, A.Yu., The mystery of two straight lines in bacterial genome statistics, e-print: <http://arxiv.org/abs/q-bio.GN/0412015> (version 2).
- [8] Gorban, A.N., Zinovyev, A.Yu., Popova, T.G., Four basic symmetry types in the universal 7-cluster structure of 143 complete bacterial genomic sequences, *In Silico Biology* **5** (2005) 0025. On-line: <http://www.bioinfo.de/isb/2005/05/0025/> .
- [9] Cluster structures in genomic word frequency distributions, Web-site: <http://www.ihes.fr/~zinovyev/7clusters> .
- [10] Lynn, D.J., Gregory A. C. Singer, G.A.C., Hickey, D.A., Synonymous codon usage is subject to selection in thermophilic bacteria, *Nucleic Acids Res.*, **30** (19) (2002), 4272-4277.
- [11] Wan, X.F., Xu, D., Kleinhofs, A., Zhou, J., Quantitative relationship between synonymous codon usage bias and GC composition across unicellular genomes, *BMC Evol Biol.* (2004) **4**(1):19.